ACS APPLIED MATERIALS & INTERFACES

Research Article

www.acsami.org

Long-Term Stabilization of Organic Solar Cells Using Hindered Phenols as Additives

Vida Turkovic,*[,†,§] Sebastian Engmann,[†] Nikos Tsierkezos,[§] Harald Hoppe,[†] Uwe Ritter,[§] and Gerhard Gobsch[†]

[†]Institute of Physics and Institute of Micro- and Nanotechnologies, Ilmenau University of Technology, 98683 Ilmenau, Germany

[§]Institute of Chemistry and Biotechnology, Ilmenau University of Technology, 98693 Ilmenau, Germany

Supporting Information

ABSTRACT: We report on the improvement of long-term stability of organic solar cells (OPV) using hindered phenol based antioxidants as stabilizing additives. A set of seven commercially available hindered phenols are investigated for use in bulk-heterojunction OPV. Polymer:fullerene films based on poly(3-hexylthiophene) (P3HT) and [6,6]-phenyl-C61-butyric acid methyl ester (PCBM) are characterized with respect to the initial power conversion efficiency and the long-term stability improvement under illumination in ambient conditions. FTIR spectroscopy is used to trace chemical degradation over time. OPV performance is recorded under ISOS-3 conditions, and an improved long-term performance of OPV devices, manifested in increased accumulated power generation (APG), is found for octadecyl 3-(3,5-di-*tert*-butyl-4-hydroxyphenyl)-propionate. Using this additive, APG is increased by a factor of 3 compared to the reference. Observed differences in the stabilization of tested additives are discussed in terms of energetic trap states formation within the HOMO/LUMO gap of the photoactive material, morphological changes, and chemical structure.

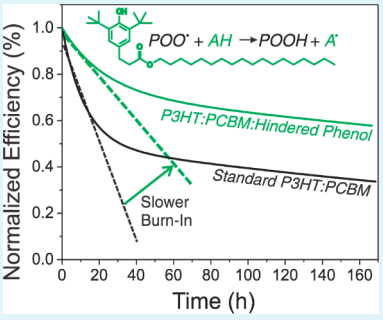

KEYWORDS: *lifetime, stabilizer, antioxidant, radical scavenger, hydrogen donor, ternary blend*

INTRODUCTION

Organic photovoltaics (OPV) has shown impressive progress over the past few years. Steady development of better materials and advanced cell architectures have made OPV more competitive with other thin film technologies, peak efficiencies have reached over 10%,[1] and the first products have been launched in the market.[2] Yet, organic solar cells are only considered exotic niche products, mostly due to a comparably poor durability and batch to batch variations of the compounds used. While batch to batch variations can easily be overcome once a large scale market is established via large scale purification of the materials, improved long-term stability is still the key to success of OPV. The long-term stability of P3HT:PCBM was subject of many investigations, especially noted here are numerous interlaboratory studies conducted by Krebs et al., who have assembled a vast long-term stability database for different OPV materials, cell architectures, testing conditions, and testing laboratories.[3] One of their most recent studies on the long-term stability of encapsulated P3HT:PCBM devices reports lifetimes in the range 0.5−40 h.[3] The lifetime of OPV devices is severely limited by photoinduced oxidation, which occurs due to UV-radiation and ingress of oxygen and water into the solar cell device.[4,5] Thus, one way to reduce degradation is to prevent water and oxygen diffusion into the device by encapsulation.[6,7] In addition, getter materials (reactive materials, which in contact with oxygen or water combine with it chemically or by adsorption, thus preventing it from reacting with the active layer materials) can be introduced to further reduce the influence of reactive species within the encapsulated device.[4,8] A second way is to effectively reduce the magnitude of photochemical changes by introducing UV-blocking layers within the sealing of the device[9] or by selecting active layer materials which are inherently more stable against oxidation.[10,11] However, it is not possible to fully prevent water or oxygen from entering the device. Materials currently synthesized to achieve high stability lag efficiency-wise behind the modern high-performing polymers,[12,13] and vice versa.[12,14] Thus, further stabilization of the active layer against chemical degradation remains a fundamental problem. In this article we present a new concept for photo-oxidative stabilization of OPV devices, by ternary blending active layers with small portions of stabilizing compounds.

EXPERIMENTAL SECTION

Materials. In this proof-of-concept study, the photochemical stability of organic solar cell active layers consisting of poly(3-hexylthiophene) (P3HT) and [6,6]-phenyl-C61-butyric acid methyl ester (PCBM) was investigated. P3HT was purchased from Rieke Metals Inc., PCBM of purity 99% was delivered by Solenne BV. P3HT:PCBM blends of mass ratio 3:2 were prepared from stock solutions, and the resulting solution concentration was 1.2 wt %

Received: April 24, 2014
Accepted: October 3, 2014
Published: October 3, 2014

   dx.doi.org/10.1021/am5024989 | *ACS Appl. Mater. Interfaces* 2014, 6, 18525−18537

Chart 1. Chemical Structure of the Investigated Hindered Phenols[a]

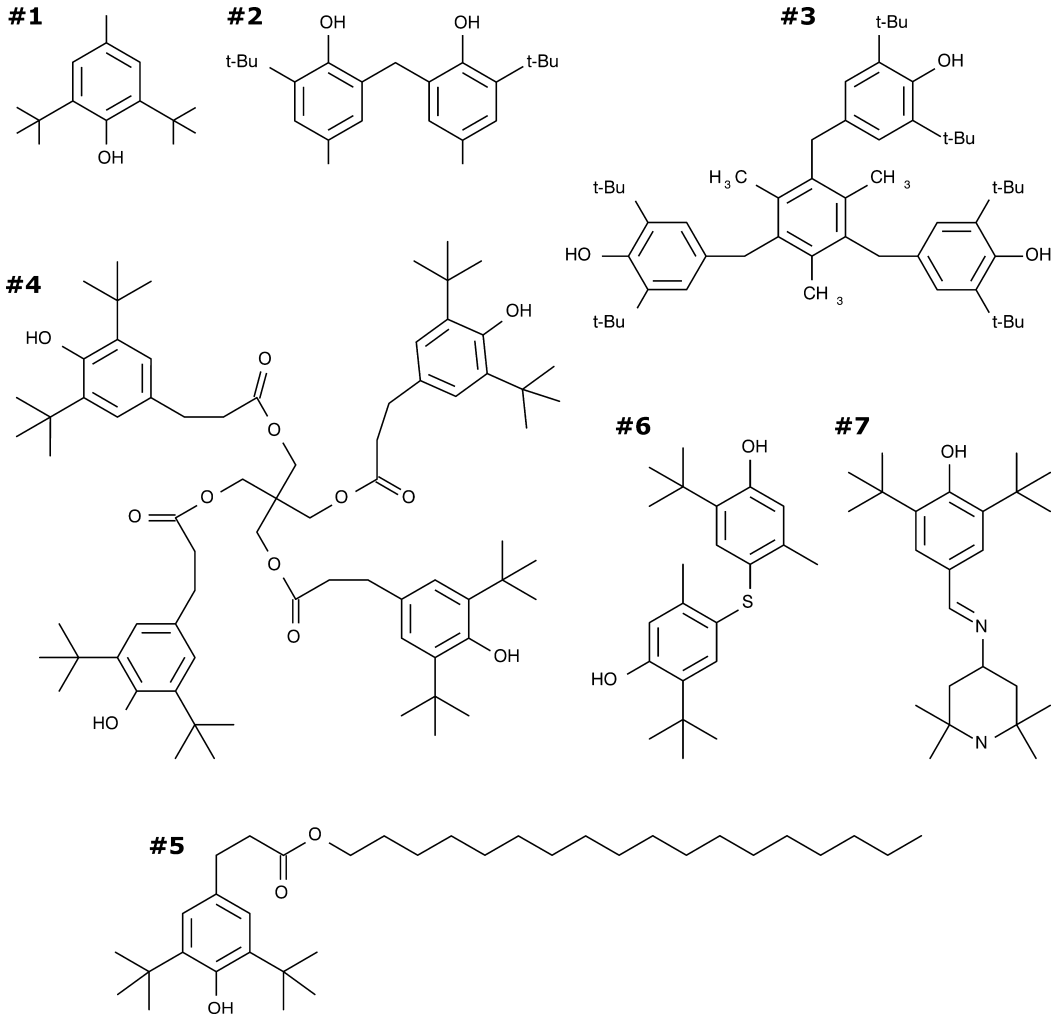

[a]For convenience, throughout the manuscript the compounds are represented by the number shown next to the structures: #1—2,6-di-*tert*-butyl-4-methylphenol; #2—2-2′-methylenebis(6-*tert*-butyl-4-methylphenol); #3—1,3,5-trimethyl-2,4,6-tris(3,5-di-*tert*-butyl-4-hydroxybenzyl)benzene; #4—pentaerythritol tetrakis (3-(3,5-di-*tert*-butyl-4-hydroxyphenyl)propionate); #5—octadecyl 3-(3,5-di-*tert*-butyl-4-hydroxy-phenyl)propionate, also known as Arenox A76; #6—4-4′-thiobis(6-*tert*-butyl-*m*-cresol); #7—2,6-di-*tert*-butyl-4-((2,2,6,6-tetramethyl-piperidin-4-ylimino)-metyl)-phenol. Optimal stabilization effect was obtained using Additive #5.

polymer in chlorobenzene. Five hindered phenols and two bifunctional stabilizers (hindered thiophenol and hindered phenol and hindered amine-HAS) (see Chart 1) were obtained from Sigma-Aldrich (#7), Reagens (#5), and TCI (the rest), and dissolved in chlorobenzene. The purity of the compounds lies in the range 95−99%.

Solar Cells. Seven hindered phenol based antioxidants, which are common stabilizers for insulating polymers, were blended in different mass concentrations with the P3HT:PCBM solution. Solar cells with active layers containing one of the seven compounds, in concentrations of 0.03%, 0.3%, 3%, 10%, and 20% of total dry weight, and reference cells with no additives added, were prepared inside the glovebox (O_2 < 1 ppm, H_2O < 1 ppm) by spin-coating on PEDOT:PSS (Clevios PH) coated ITO/glass substrates (previously annealed in ambient at 140 °C for 20 min). The thickness of the active layers was set to 100 nm. Prior to the evaporation of the aluminum cathode, the films were annealed at 160 °C for 10 min (precathode annealing). An approximately 150-nm-thick cathode was deposited under high vacuum (base pressure smaller than 5×10^{-6} mbar) via thermal evaporation. Completed solar cell devices were encapsulated behind glass inside the glovebox using a UV curable epoxy glue DELO LP 655. The parameters of the as-cast devices, short circuit current density (J_{sc}), open circuit voltage (V_{oc}), fill factor (FF), and power conversion efficiency (PCE), were extracted from $J(V)$ characteristics, which were recorded under AM 1.5 conditions using a Keithley SMU 2400. Do note that the solar cells were pre-cathode annealed to ensure comparable morphologies of the films and the devices. Due to these differences in morphology (a thin layer of face-on P3HT is formed on top, representing a barrier to electron transport), the V_{oc} and thus the efficiencies are lower than in the case of post-cathode devices.[15] Accelerated long-term stability testing under continuous light illumination (1 kW/m^2) were performed according to ISOS-3 standards[3] using a homebuilt setup.[16] The solar cell parameters were traced in situ for more than 100 h via periodic $J(V)$ measurements. Reported values refer to arithmetic averages of four solar cells.

Spectroscopy. Polymer:fullerene films were prepared in a similar manner as reported for the solar cell devices, but on CaF_2 substrates. Such prepared films were characterized via Fourier transform infrared (FTIR), UV−vis, and photoluminescence (PL) spectroscopy, before and after their degradation inside the stability setup used for solar cell characterization. FTIR spectra were recorded using a JASCO FT/IR-4000 Series spectrometer. Transmission (T) and reflection (R) spectra in the wavelength range 300−800 nm were recorded using Agilent Cary 5000 UV−vis-NIR spectrometer. The film absorption (A) was calculated via $A = 1 - T - R$, neglecting any light diffraction. PL-spectra were recorded using Avantes SensLine spectrometer AvaSpec-ULS2048XL. The excitation wavelength was 445 nm.

Cyclic Voltammetry. In order to determine the redox potentials of the compounds used, namely, electrochemical energy levels indicating possible trap states with respect to the HOMO/LUMO of P3HT:PCBM, cyclic voltammetry measurements were performed. For this purpose, the compounds were dissolved in dichloromethane containing *n*-tetrabutylammonium hexafluorophosphate (TBAPF6) as the supporting electrolyte. The concentration of the supporting electrolyte TBAPF6 and the investigated compounds was 0.1 mol/L and 10^{-3} mol/L, respectively. The electrochemistry measurements were performed on electrochemical working station Zahner IM6/6EX. The obtained results were analyzed by means of Thales software (v 4.15). A three electrode system consisting of glassy carbon working electrode, platinum counter electrode, and Ag/AgCl (0.1 M NBu_4Cl, acetonitrile) reference electrode, was used for the electrochemistry measurements. All potential values are reported versus Ag/AgCl (0.1 M NBu_4Cl, acetonitrile) reference electrode. The cyclic voltammograms were recorded at the scan rate of 0.05 V/s at room temperature. More details concerning the electrochemistry experiments were already reported in previous published articles.[17−19] The trap levels of each of the additives were determined via the empirical relation $E_{Trap} = (E_{onset} + 4.35)$ eV, where E_{onset} is the onset of the reduction or oxidation peak, 0.45 V is the value for ferrocene vs Ag/AgCl, and 4.8 is the energy level of ferrocene below the vacuum. In the case of the materials that could not be reversibly oxidized, the potential given is the irreversible anodic peak potential, the first peak of the CV trace. It must be noted here that an irreversible peak potential may correspond to within 100 mV of the reversible oxidation potential if the species generated by a reversible electron transfer process is consumed by a rapid, chemical follow-up reaction.[20,21]

RESULTS AND DISCUSSION

We report on the use of stabilizing additives for stabilization of OPV against photo-oxidation, thus extending the long-term stability of encapsulated solar cells. For that purpose, hindered phenol based antioxidants, which are common stabilizers for commercial insulating polymers, were blended in different mass concentrations into the polymer:fullerene mixture. In this proof-of-concept study, we are demonstrating that not every stabilizing additive causes an improvement of the long-term performance of the solar cell device, and discuss the conditions that have to be met for their successful implementation. For the tested reference system P3HT:PCBM, only one of the seven tested hindered phenols, namely, octadecyl 3-(3,5-di-*tert*-butyl-4-hydroxy-phenyl)propionate, has shown the ability to significantly increase the long-term stability under ISOS-3 conditions[22] of encapsulated OPV devices, increasing the accumulated power generation by a factor of roughly four as compared to reference devices with no additive added.

Sterically Hindered Phenols. The additives introduced into the P3HT:PCBM system are shown in Chart 1. These compounds belong to the chemical group of sterically hindered phenols, and they are commonly used stabilizers for commercial polymers, such as polyolefins, rubber, styrenic polymers, polyesters, polyamides, polyacetals, polycarbonates, polyurethanes, and so forth.[23]

In contact with air and light, the polymer reacts with oxygen, which produces different oxidized polymer species and breaks the polymer chain, leading to irreversible failure in functioning of the devices.[24,25] Recently it has been shown by Hintz et al. that two concurrent mechanisms take place in the degradation process, depending on the irradiation conditions.[26] Under the UV irradiation, the degradation proceeds as a radical reaction[24,25] starting at the α carbon of the alkyl side chain, and results in simultaneous degradation of the π conjugated system and the side chain. Under visible illumination, however, the reaction involves a photosensitized species, possibly singlet oxygen[26,27] that primarily destroys the π conjugated system of the polymer, leaving the side chain almost unaffected. In white light conditions, both of the mechanisms are active, but since the radical chain mechanism has a higher effectiveness, it dominates even though only a low UV irradiation fraction is present.[26]

The generalized scheme of polymer degradation, as first developed by Bolland and Gee,[28] and the degradation inhibition mechanism[29] via hindered phenols are depicted in Scheme 1. It is considered that the degradation starts via

Scheme 1. General Polymer Degradation Mechanism and Stabilization Using Hindered Phenols

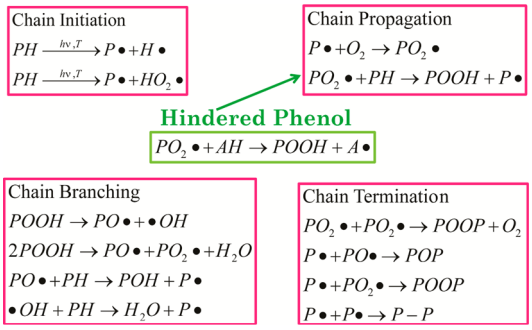

adventitious catalysts, such as transition metals, radical initiators, impurities in the monomers, and minute amounts of oxygen, which are included in the polymer in course of polymerization.[23] Upon reaction of these impurities with the polymer, peroxy radical POO● is formed, which abstracts hydrogen from the polymer and forms and alkyl radical P●. It reacts with molecular oxygen practically without any activation energy, forming additional peroxy radical POO●. Subsequently they form hydroperoxides POOH upon abstraction of hydrogen.

In the presence of hindered phenols (denoted with AH in Scheme 1), the rate of this reaction, defined by the activation energy needed to abstract the hydrogen from the polymer, competes with the rate of abstraction of substantially more abstractable hydrogen from the hindered phenol.[29] The stability of the phenoxyl radical created from the additive is influenced by the steric hindrance of the hindered phenols (*tert*-butyl groups in the 2- and/or 6-position), preventing them from reacting with the polymer and from dimerization with other phenoxyl radicals. The labile hydroperoxides are then further decomposed into highly reactive radicals, alkoxy PO● and hydroxyl ●OH. In the last step, the formed radicals recombine among themselves, leaving behind inert product, thus terminating the degradation process.[23]

Ternary Blends. *Electronic Trap States.* As organic solar cells are optoelectronic devices, the energy levels (HOMO/LUMO) of each of the constituents of the bulk-heterojunction are of fundamental importance for the device performance. Besides the LUMO (HOMO) offset necessary for the photoinduced charge transfer between the polymer and fullerene, the energetic position of any additional blend constituent might impair the maximum reachable power conversion efficiency (PCE).[30,31] Gap states/trap states E_{trap}, within the effective band gap of the photoactive layer $E_{gap,eff} = E_{LUMO}^{Acceptor} - E_{HOMO}^{Donor}$, are centers for nongeminate recombination of free charge carriers. The recombination rate of electrons

$R_{e,trap}$ (holes $R_{h,trap}$) via trapped holes (electrons) can be given in the form

$$R_{e,trap} = \frac{\beta_e q \mu_e}{\varepsilon} n p_{trapped} \quad (1)$$

$$R_{h,trap} = \frac{\beta_h q \mu_h}{\varepsilon} p n_{trapped} \quad (2)$$

where μ is the charge carrier mobility, $n(p)$ the electron (hole) density, and $p_{trapped}$ ($n_{trapped}$) the density of trapped holes (electrons). The dimensionless factor β corresponds to the probability of a free charge carrier to find a trap level and is therefore strongly morphology dependent. A strong chemical incompatibility and resulting decomposition of the blend matrix might lead to the formation of large agglomerates with high trap density, but at the same time to a reduction of the probability for free charge carriers to find those traps as the effective interface area decreases. This is due to the localized charge transport via hopping, which is in contrast to delocalized band transport of free charges in classical semiconductor physics, e.g., silicon solar cells. For this reason, the well-known Shockley-Read-Hall (SRH) recombination found in classical semiconductors cannot be used in a one to one manner on organic solar cell devices, but might be used to give useful guidance. Similar to the case of SRH recombination, photogenerated charges, generated at rate G, are captured by localized trap states with the rates $R_{e,trap}$ and $R_{h,trap}$, and are thermally emitted with rates $G_{e,trap}$ and $G_{h,trap}$ back to the LUMO and HOMO of the active layer; see Figure 1.

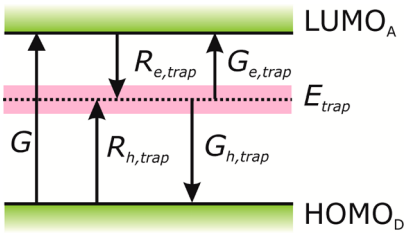

Figure 1. Electrons and holes produced by the photoinduced charge transfer are captured by a trap level E_{trap} with the rates $R_{e,trap}$ and $R_{h,trap}$. Electrons (hole) occupying the localized trap state can be thermally emitted back to the acceptor LUMO (donor HOMO) with rate $G_{e,trap}$ ($G_{h,trap}$).

Following Boltzmann statistics, the generation from trap states or detrapping G_{trap} depends exponentially on the energetic position of the trap state with respect to the HOMO of the donor (that is, LUMO of the acceptor) of the photoactive material

$$G_{e,trap} \propto n_{e,trap} \exp\left[-\frac{E_{LUMO}^{Acceptor} - E_{trap}}{k_B T}\right] \quad (3)$$

$$G_{h,trap} \propto p_{trap} \exp\left[-\frac{E_{trap} - E_{HOMO}^{Donor}}{k_B T}\right] \quad (4)$$

Thus, at room temperature holes or electrons which were trapped in an energetic state near the middle of the effective band gap or just far away from either the donor HOMO or acceptor LUMO, most likely stay localized until their recombination with a free charge carrier. Thus, trap states close to the middle of the band gap will possibly lead to the biggest loss of free charge carriers and a reduction of the maximum short circuit current and open circuit voltage.

Figure 2 shows the photovoltaic parameters dependent on concentration of Additive #7. The strong exponential decay in all of the parameters even at relatively small concentration (up to 3%) suggest that the cause might be the introduction of a trap level.

The cyclic voltammogram of this compound, shown in Figure 3a, revealed a −4.06 eV LUMO level, and an additional oxidation peak with an onset at −4.6 eV. As the optical band gap was estimated from Figure 3b to 2.8 eV, thus giving a HOMO level of −6.89 eV, we attribute the small oxidation peak to impurities[32,33] (various synthesis residue catalysts[34,35] and defects[36]) within the additive.

Note, in Figure 4, that the trap level is ∼0.4 eV lower than the LUMO of PCBM and 0.4 eV bigger than the HOMO of P3HT. Thus, the Additive #7 forms deep trap states within the effective band gap of the active layer. Already at a low concentration (0.3%) of added Additive #7, solar cells have a power conversion efficiency prior to degradation, PCE_0, of 0.02% (compared to 1.48% for the reference device without additives), due to a significant reduction of the open circuit voltage to 109 mV compared to 389 mV of the reference solar cells without additives. This reduction of the V_{oc} is in perfect agreement with the considerations above, which predict a reduction of the open circuit voltage for traps near the band gap

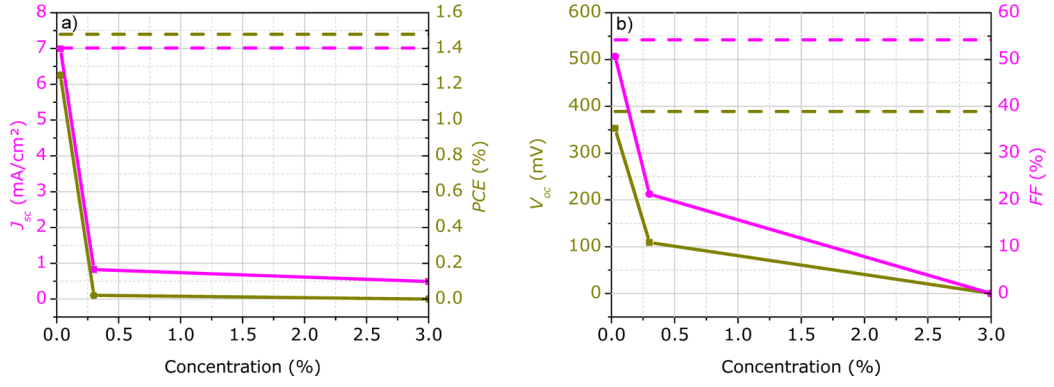

Figure 2. Photovoltaic parameters dependent on concentration of Additive #7 in the active layer, (a) short circuit current (dark red squares) and efficiency (green circles), (b) open circuit voltage (blue squares) and fill factor (magenta circles). The parameters of the reference device (with no additive added) are represented, respectively, by colored lines.

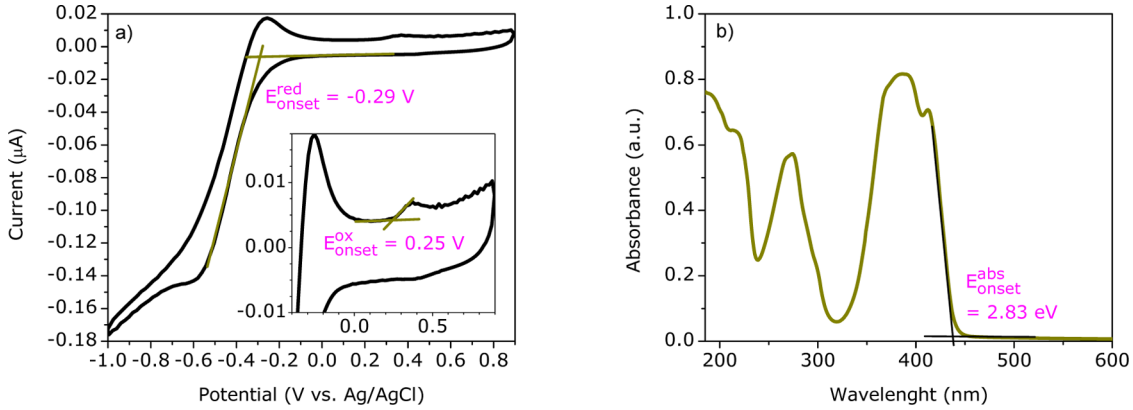

Figure 3. (a) Cyclic voltammogram of compound #7 in a dichloromethane solution containing 0.1 mol/L of the supporting electrolyte *n*-tetrabutylammonium hexafluorophosphate (TBAPF6). The potential is given with respect to the Ag/AgCl reference electrode; the scan rate was 50 mV/s. (b) Absorption spectrum was used to determine the optical band gap. UV−vis absorption was measured on thin films spin coated on a CaF_2 substrate.

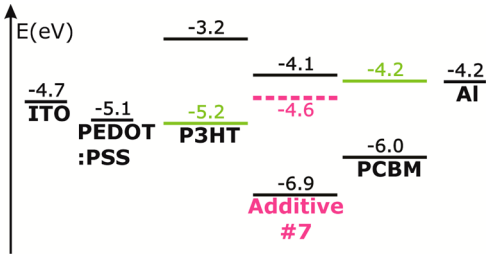

Figure 4. Energetic position of the electrochemical level of Additive #7, in comparison to the HOMO and LUMO levels of the photoactive blend P3HT:PCBM. Values are given with respect to the vacuum energy. The dotted level in the gap of Additive #7 represents the trap level.

middle, and visualizes the importance of the knowledge of the energetic levels of each of the blend constituents. A morphological problem due to the addition of the additives could be excluded in all of the cases (see Discussion)

Morphological Issues. The second highly important point that has to be taken into account when analyzing the solar cell performance is the influence of an additional third compound on the morphology of the binary blend. In order to achieve an optimum trade-off between charge separation, charge transport, and charge extraction, small amounts of stabilizing additives are often used. Although their role is limited only to interaction with the blend constituents in liquid phase, and upon drying they are expected to have left the active layer, they can drastically alter the blend morphology.[37] In our case, we are adding solid compounds which stay in the active layer (for further details, please refer to the Table SI4 and Figure SI3 in the Supporting Information), thus creating a ternary blend. The thermodynamic interactions between the components in a ternary blend are significantly more complex; thus, changes in morphology, which will in turn affect the performance of the devices, might occur.[38,39]

Figure 5 shows the experimentally measured photoluminescence signal, as well as the AFM (atomic force microscopy) topography of the reference P3HT:PCBM film compared to the film containing one of the hindered phenols (Additive #7), both measurements obtained prior to degradation.

AFM measurements suggest quite similar film topography, and presumably the bulk; thus, the cause of the slightly lower photoluminescence signal of the film containing Additive #7

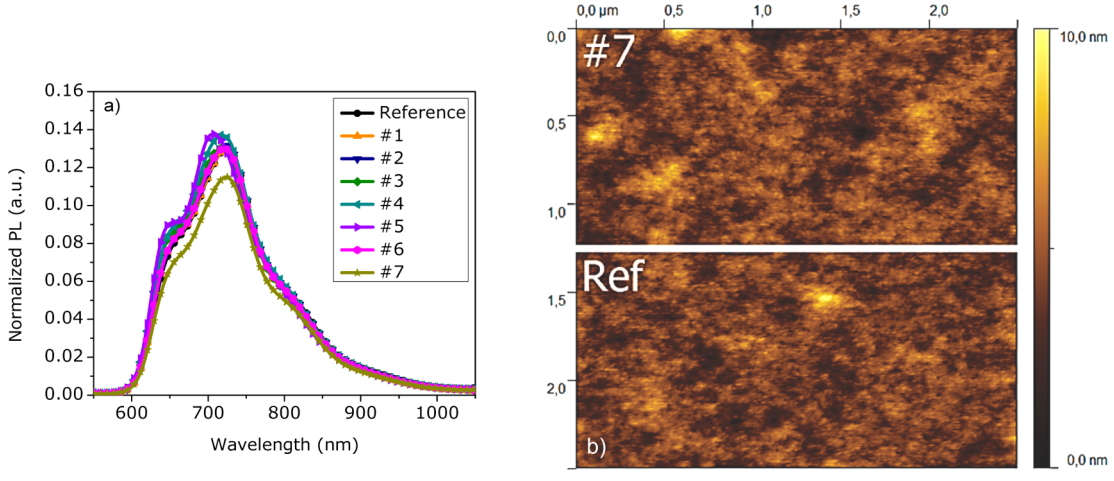

Figure 5. (a) Photoluminescence signal of P3HT:PCBM nondegraded films containing each of the seven hindered phenols (concentration as noted in Table 1), as well as the reference without any additive. The PL excitation wavelength was 445 nm (~2.78 eV), which is below the optical gap of each of the additives. (b) AFM topography image of the reference film and of the P3HT:PCBM film containing compound #7.

dx.doi.org/10.1021/am5024989 | *ACS Appl. Mater. Interfaces* 2014, 6, 18525−18537

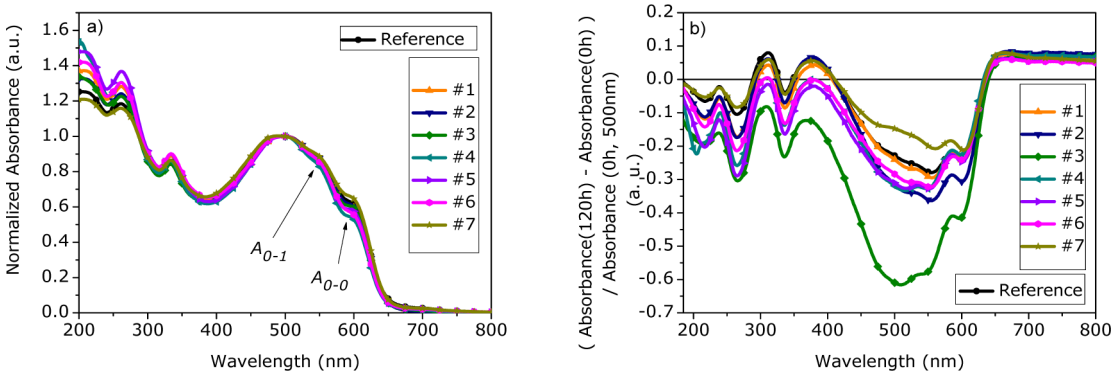

Figure 6. (a) Normalized UV−vis absorption spectra of the nondegraded films with additives and one reference with no additive on CaF substrates. Normalization was done with respect to the absorption peak at around 500 nm. (b) Relative change in absorption of the films after 120 h of continuous 1000 W/m^2 illumination in ambient. Note that all spectra were normalized to the absorption peak at 500 nm of the corresponding nondegraded film.

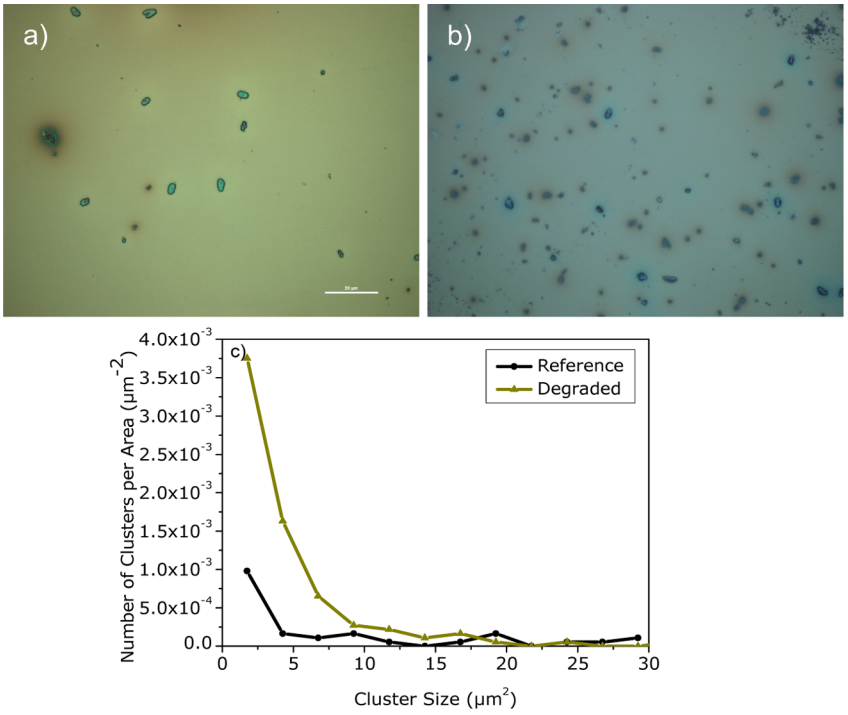

Figure 7. Optical microscope images of the reference film: (a) as-cast, (b) after 5 days of degradation under illumination (1000 W/m^2, ambient). (c) Frequency count of the cluster size for both samples.

compared to the reference and the rest of the films with hindered phenols is not expected to be morphology-related. However, as AFM can only probe the surface morphology, further measurement techniques such as scattering methods,[40−42] differential scanning calorimetry,[43] or 3D tomography[44] are needed to confirm the exact morphology of the bulk.[41,42,45,46] Nevertheless, since the performance of most of the solar cells containing additives is comparable to that of the reference cells (see Supporting Information Table SI3), knowing the exact detailed morphology of the active layer morphology is not necessary for investigating the role of hindered phenols on the stabilization of OPV, and relevant information can be obtained indirectly using UV−vis and PL spectroscopy and IV measurements. However, in general, compounds other than those reported within this manuscript might cause significant morphological changes, and thus affect the solar cell performance more drastically.

Two possible factors might explain the observed lower photoluminescence signal. First, its bandgap, unlike that of the rest of the additives, reaches further in the visible spectra (see Supporting Information Table SI1). As the normalization was done with respect to the excitation laser wavelength, and the absorption of the film in that region is additionally higher due to the absorbance of the additive, the normalization might result in an underestimation of the photoluminescence. The other possibility is that the additive is capable of acting as an additional excitation quencher. This interpretation is further supported by a fill factor >50% of the solar cells containing Additive #7 (see Supporting Information Table SI2), which is comparable to the reference solar cell. In case the additive acted as a compatibilizer for P3HT and PCBM, causing a finer intermix of both components across the blend, a much smaller FF would be expected, due to a drastic increase of the recombination of charge carriers and the buildup of space

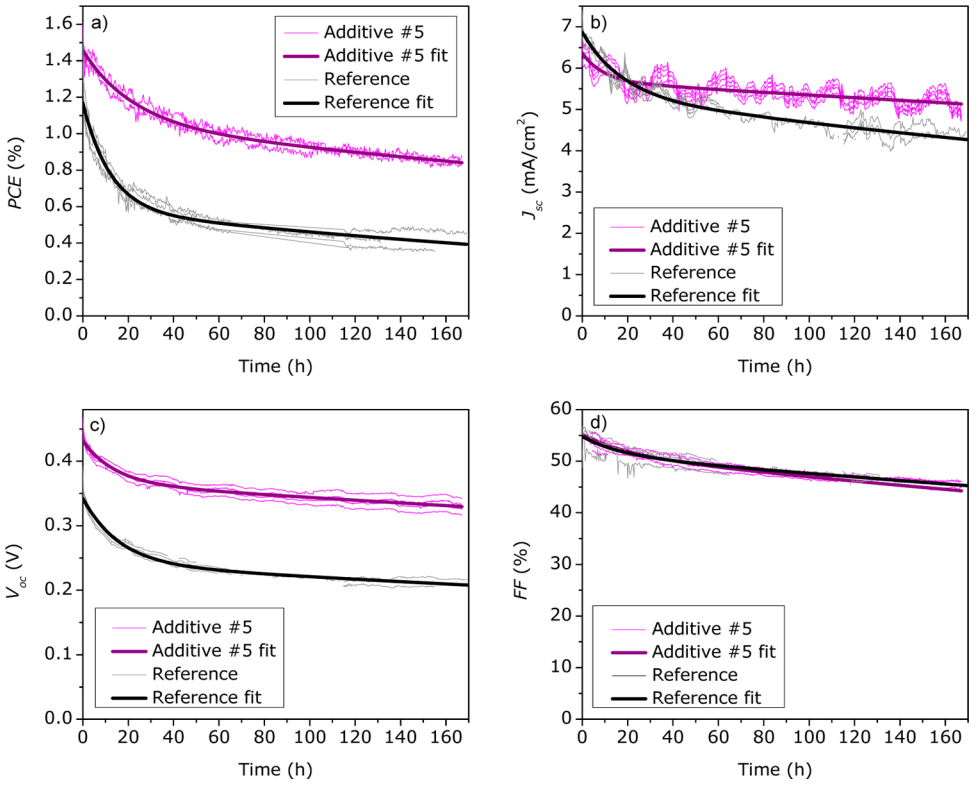

Figure 8. Long-term (a) PCE, (b) J_{sc}, (c) V_{oc}, and (d) FF of solar cells without additives and containing hindered phenol #5 as a function of stressing time, for a set of four solar cell devices. The solar cells were measured continuously during 1000 W/m^2 illumination of a metal halide lamp. The time dependence of the parameters was fitted using a biexponential decay curve, by least-squares-fitting of measured cells. In order to avoid the effect of day-to-day variations in humidity and room temperature, all devices were measured in a fully automated test setup. The inhomogeneity of the illumination was measured to be within 10% of the nominal value.

charges.[45,46] The relatively unchanged morphology of the blend, especially the degree of polymer order, was further supported by UV−vis measurements in Figure 6.

Bleaching. Blend films containing one of the seven hindered phenols and a reference film without additive were prepared on CaF substrates. Freshly prepared and degraded films were investigated via UV−vis and FTIR spectroscopy to elucidate the effect of the antioxidant on the blend degradation upon direct illumination in ambient conditions. Note that the active layer was not shielded from UV-radiation during aging. Figure 6 shows the normalized absorption spectra of all investigated films prior to degradation in air, as well as the relative absorption change upon film aging. In agreement with the morphology results reported above, the polymer order within all films stays unaltered independent of the stabilizing additive compared to the reference device, which is manifested in a nearly identical ratio of the A_{0-0} and A_{0-1} absorption peaks, and a good overlap of the absorption spectra in the wavelength range 300−800 nm after normalization to the maximum polymer absorption. Since all additives have shown large optical band gaps (see Supporting Information Table SI1), the blend absorption for each of the investigated films only differs in the high energy region.

While there is no significant difference observable for the freshly prepared films, this changes drastically upon degradation. After 120 h of film aging under 1000 W/m^2 continuous light illumination in air, all of the films show significant photobleaching; see Figure 6b). The bleaching of the ground state polymer absorption (S_0−S_1 transition) due to formation of a charge transfer complex between O_2 and the polymer in early degradation stages,[47] as well as due to the creation of a photo-oxidized polymer species,[24,25] can be observed in the wavelength range 450−650 nm. Below 450 nm the "bleaching" is a consequence of a simultaneous morphological degradation including the formation of large fullerene clusters at elevated temperatures[40,48−50] and additional photochemical degradation of the fullerene derivative.[51,52] The newly formed absorption band (above 650 nm) upon illumination was recently interpreted as the high energy electronic absorption (P_2 band) of P3HT corresponding to the D_2−D_0 transition of the polymer radical cation.[47,53−55] A second interpretation, more relevant for our samples, is the increase of light scattering due to morphological changes and the formation of PCBM clusters during degradation. Figure 7 shows the optical microscopy images of the reference film without the additive prior to and upon degradation, to support this conclusion.

All of the films are significantly bleached upon degradation. As all of the tested additives are known to work as antioxidants in other polymer systems, these results might be somewhat unexpected, since photobleaching is attributed to the breaks in conjugation,[24,56] and in the case of P3HT it was found that the magnitude of absorption decrease is directly proportional to the number of oxidized thiophene rings.[56]

Tested phenols suffer from a significantly higher bleaching of the active layer in the visible wavelength range compared to the reference film without the additive. This suggests increased thiophene ring destruction in the presence of the additives. Indeed, it was reported that the contribution of some products of consumption of hindered phenols that arise during polymer lifetime as a consequence of reactions with alkylperoxy radicals,

principally the ultimate transformation products quinone methides,[57,58] to discoloration of stabilized plastics during aging.

It was shown in a study by Hintz et al. that, depending on the irradiation wavelength, two different degradation mechanisms will take place, each attacking different parts of the polymer.[26] Hindered phenols are preventing the radical degradation pathway[24] which affects both alkyl side chains and the conjugated π system, but have no effect on the degradation via photosensitized species which primarily attacks the conjugated π system.[27] This explains why films that are protected by hindered phenols from the highly effective free radical attack still exhibit photobleaching.

It was already reported in MDMO-PPV cells that the loss in absorbance is not the main factor responsible for the decrease in performance upon photooxidative degradation.[59] As photobleaching is a consequence of the loss in conjugation and thus backbone degradation, the side chain reactions do not contribute to the visual impression of degradation which is observable in simple UV−vis measurements; however, they will be of significant electronic importance.

This becomes clear considering two things. First, the absorption and thus extractable current density is more or less linearly dependent on the concentration of absorbers and their absorption coefficient. Second, the recombination rate of free charge carriers and excitons depends on the probability of finding traps or defects. If we assume that radicals and later stage degradation products lead to exciton trapping and recombination, due to a strong electron pulling effect, the number of extractable charges is proportional to the probability that no traps can be found. In the case of homogeneously distributed traps (volume concentration c_t), the latter one can be expressed by the Poisson probability

$$p = \exp(-Vc_t) \tag{5}$$

where V is the via diffusion accessible volume of the exciton. Indeed, Bauld et al. found an exponential relationship between the solar cell efficiency and paramagnetic defect (radical) density.[60]

By these considerations we want to emphasize that the visual appearance is not necessarily a good indication of the device performance. Additional measurements yielding information about the fraction of reaction products are therefore of utmost importance. Furthermore, optical results should be always compared to the actual device performance.

Long-Term Stability. After investigating the optoelectronic and morphological properties of the P3HT:PCBM films containing hindered phenols, solar cells containing each one of the seven antioxidants were tested with respect to the stability enhancement of the solar cells compared to reference solar cells without additives. Encapsulated pre-cathode annealed solar cells were stressed for 150 h under accelerated degradation conditions. In Figure 8 the solar cell parameters during continuous illumination of 1000 W/m^2 of the reference cell without additives and the best stabilized cell containing Additive #5 are compared.

In the investigated samples only two time regimes were observed; thus a biexponential decay in the form

$$\mathrm{PCE}(t) = a_1 \cdot \exp\left(-\frac{t}{t_1}\right) + a_2 \cdot \exp\left(-\frac{t}{t_2}\right) \tag{6}$$

was used to quantitatively describe the time dependence of the photovoltaic parameters during illumination.[61]

Two values, $t_{\text{burn-in}}$ and t_{life}, for the burn-in period and the lifetime of the solar cell, respectively,[62] are extracted from the fitted curves for the purposes of evaluating the stability of the solar cells. The burn-in of the PCE is characterized by a fast decay, described by the time constant t_1, while t_2 corresponds to a slow degradation process of the solar cell following the burn-in. However, there is no exact rule on how to derive these parameters, and the burn-in period is commonly approximated by a point in time where the dynamics of the decay changes. In this study, we analytically define the burn-in time as the intersection between the first derivations of the two exponential contributions of the fitted curve

$$t_{\text{burn-in}} = \ln\left(\frac{A_2 t_1}{A_1 t_2}\right)\frac{t_2 t_1}{t_1 - t_2} \tag{7}$$

Thus, in order to interpret the effect of the additive on the stabilization of the OPV device, we defined an additional parameter, APG, which can be calculated to reflect commercially relevant information concerning the power which can be generated by the device. Accumulated power generation (APG) is calculated as the integral of extrapolation of PCE measured under continuous illumination (1 kW/m^2) for a given period of time (two years), as depicted in Figure 9.

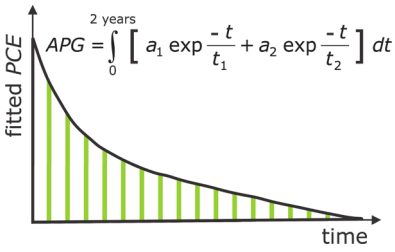

Figure 9. Graphical representation of accumulated power generation APG.

This parameter incorporates the initial and final power conversion efficiency in one parameter, thus taking into account that a device with initially slightly lower PCE can compensate for it with a slower decay of the PCE, resulting with a higher power accumulation throughout their lifetime.

In Table 1 the determined long-term performance of the solar cells with and without additives is given in the form of biexponential fit parameters a_1, a_2, t_1, and t_2, percentage ratio of the final and initial efficiency $\mathrm{PCE}_{\text{end}}/\mathrm{PCE}_0$, $t_{\text{burn-in}}$ and t_{life} values, and APG.

It becomes obvious that only one of the seven tested hindered phenols is suitable for an application as stabilizer for organic solar cell devices. The use of octadecyl 3-(3,5-di-*tert*-butyl-4-hydroxyphenyl)propionate, also known under the product name Arenox A76, lead to an increase of the accumulated power generation by a factor of 3 compared to the reference device without additive, while all other tested compounds did not improve the stability of the active layer.

The increase of the APG obtained with Additive #5 is caused by a simultaneous increase of the burn-in time as well as an overall slower decay of the PCE (compare t_1 and t_2 values with those of the reference device and all other additives). Note also that the ratio a_1/a_2 is significantly smaller compared to all other devices (#5—0.4 compared to ∼1 for all other cases). This is

Table 1. Solar Cell Long-Term Performance for Devices with and without Additives[a]

#	conc. [%]	PCE_0 [%]	a_1	a_2	t_1 [h]	t_2 [h]	$t_{burn\text{-}in}$ [h]	t_{life} [h]	$PCE_{burn\text{-}in}$ [%]	PCE_{end} [%]	PCE_{end}/PCE_0 [%]	APG_{2yrs} [kWh/m^2]
1	20	1.26	0.36	0.57	14.0	331	40	61	0.53	0.34	27	194
2	20	1.30	0.38	0.63	15.1	321	40	57	0.58	0.37	29	208
3	10	0.87	0.34	0.24	9.4	186	33	30	0.21	0.10	11	48
4	20	1.55	0.62	0.55	10.7	170	33	28	0.48	0.20	13	100
5	**20**	**1.57**	**0.40**	**1.05**	**22.3**	**742**	**58**	**142**	**1.00**	**0.84**	**53**	**788**
6	20	1.23	0.53	0.47	21.5	289	63	49	0.41	0.26	21	147
7	0.03	1.25	0.38	0.46	14.4	354	45	65	0.42	0.29	23	168
ref		1.48	0.59	0.58	12.2	434	45	85	0.54	0.39	27	259

[a]Note that optimization was done with respect to the maximum obtainable additive concentration yielding a PCE which is not smaller than 2/3 of the reference's PCE (see Supporting Information Table SI3). Also note that the cells were pre-cathode annealed. Reported values refer to the arithmetic average of 4 solar cells. Shown are the calculated parameters of the bi-exponential fit, a_1, a_2, t_1, and t_2, as well as the commonly used $t_{burn\text{-}in}$ and t_{life} time. The power conversion efficiency after the burn-in ($PCE_{burn\text{-}in}$) and the power conversion efficiency after the end of the test period of 168 h (PCE_{end}) are shown for completeness. The extrapolated accumulated power generation after two years of continuous illumination with 1 kW/m^2 (APG_{2yrs}) is used as assessment for the stabilization effect. Highlighted in bold is the row with the devices having APG value higher than the reference, stabilized with Additive #5.

equivalent to a significantly decreased loss of the PCE during the burn-in period. Furthermore, this result indicates that the dominant degradation mechanism of the active layer might have changed compared to the reference device.

The activity mechanism of hindered phenols is based on hydrogen transfer from the phenolic hydroxy group to alkylperoxyls derived from polymers oxidizing by a chain breaking mechanism.[29,63] The primary transformation products are phenoxyl radicals A$^\bullet$, which play a key role in the chemistry of phenolic antioxidants, and are the precursors of all further transformation products. In the course of aging, the activity of the additive gets depleted, in interactions with alkylhydroperoxides, photolysis, sensitized photooxidation, and impurities (such as transition metal ions).[29,63] Essential bimolecular processes are depicted in more detail in Scheme 2, and include disproportionation to quinone methide (QM) and starting phenol (InH) (route a), that is, regeneration of antioxidant and formation of R$^\bullet$ trap (route d and e); C−O and C−C couplings leading to aryloxycyclohexadienones (ArO−CHD) and phenolic dimers (HIn$^\bullet$−$^\bullet$InH); and recombination with $RO_2^\bullet$ to alkylperoxycyclohexadienones (ROO−CHD) (route c).[64]

The transformation products of the phenols can also possess antioxidant or even radical scavenging abilities, as in the case of propionate type phenolics (various derivatives of 3-(3,5-di-*tert*-butyl-4-hydroxyphenyl)propionic acid), such as Additives #4 and #5, which makes them superior to the other types of hindered phenols. The effect is based on an intermolecular rearrangement and aromatization of the conjugated QM system.[64] As shown in Scheme 3, the initial additive is prone to aromatization to a phenolic cinnamate, a strong antioxidant. In reactions with alkylperoxy radicals, dimeric quinone methide is formed, which can rearrange to a phenolic cinnamate dimer, which is capable of scavenging alkylperoxyls. In the ultimate phase, a conjugated quinone methinoide dimer is formed. Analogous transformations also take place in polynuclear propionate phenolics, such as Additive #4.[63] However, the other tested compound from this group, Additive #4, exhibited a much lower stabilization effect. We suggest that its bulky structure might be the cause for it, as it is known to limit the solubility of the additives in insulating polymers.[65,66] This would result in a nonhomogenous dispersion throughout the active layer, which in turn reduces the active layer fraction which is in contact with the additive and can thus be stabilized.

Scheme 2. Essential Bimolecular Processes of Hindered Phenols (Adapted from Pospisil et al.[64])

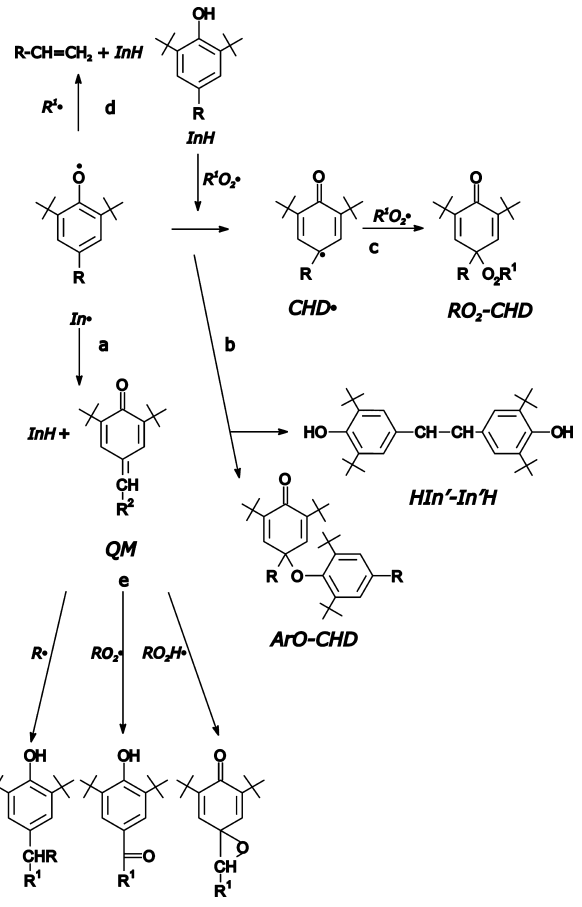

Similar observations can be made in the subclass of partially hindered benzyl phenols, which have substituents at least in 4- (or 2- or 6-) position having H atoms on a C atom vicinal to the phenyl group,[23,63,67] such as Additives #1, #2, and #3. Since the hydroxyl group of the phenol is the active hydrogen donor, one would expect that the stabilizing effect of an additive is in direct correlation with the number of available phenol groups within the additive. However, stronger efficiency loss after 1 week of degradation of Additive #3, as compared to Additives #1 and #2, as shown in Table 1, suggests, as in the case of

Scheme 3. Transformation Products of Propionate Type Phenolics (Adapted from Pospisil et al.[63])

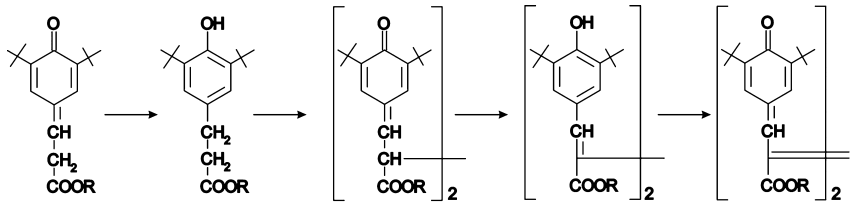

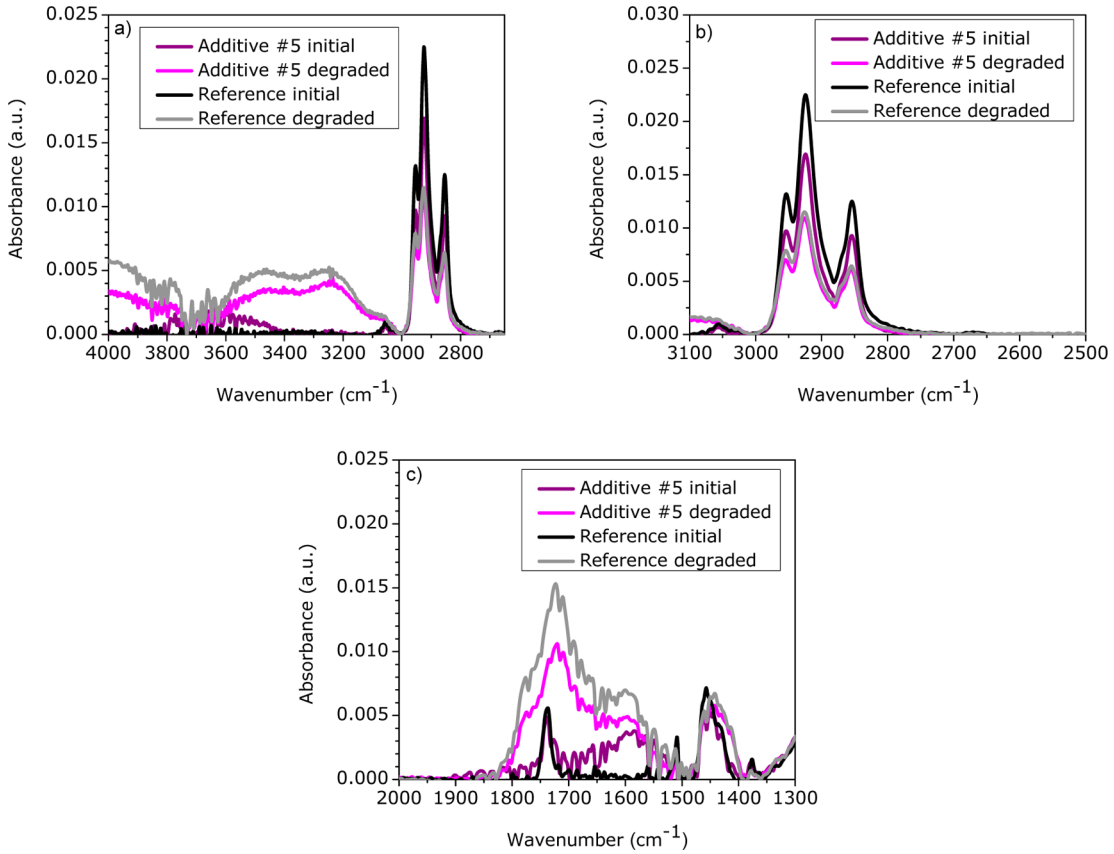

Figure 10. FTIR spectra of the samples containing Additive #5 and reference samples with no additive: (a) hydroxyl region, (b) carbonyl, (c) fingerprint region.

Additive #4, that the stabilization effect might be limited by the bulkiness of the stabilizer. The origin of the PCE decay, the degradation mechanism, cannot be resolved from the PCE measurements alone, and other measurements are needed. Imaging techniques are mentioned here such as photo/electroluminescence imaging, dark-lock in thermography[16] of solar cells, as well as Fourier transform infrared spectroscopy (FTIR) or UV–vis absorption spectroscopy[24,56] and photoelectron spectroscopy[68] or time-of-flight secondary ion mass spectrometry analysis in conjunction with isotopic labeling of degraded thin films,[69] in order to resolve whether the degradation of the electrodes, photo-oxidation of the photoactive layer, or formation of defect states are the main degradation factors.

From the considerations in previous sections and the above-mentioned structural characteristics, we suggest that the increase in long-term performance using Additive #5 is occurring via a reduction of radical states and reduced exciton recombination. To confirm this, we measured the reference and degraded (AM 1.5 illumination in air) samples with FTIR, as shown in Figure 10. As identified in the study by Manceau et al., the peak arising at 3460 cm^{-1} in the spectra of degraded samples is attributed to hydrogen-bonded –OH stretching of alcohols and hydroperoxides.[24] These products correspond to the products formed in the chain propagation step, in reaction of peroxy radicals with the polymer, which yields hydroperoxides and alkyl radicals, as depicted in Scheme 1. As seen in Figure 10a, the intensity of these peaks in the sample containing Additive #5 is lower, which is consistent with the above-mentioned characteristic of partially hindered phenols to form quinone methides, which by reacting with alkyl and peroxy radicals in the chain propagation step can reduce the amount of hydroperoxides formed. As a consequence, less of the reactive alkoxy and hydroxyl radicals will be formed in the chain branching step, and those which will be formed will partially also react with the additive-borne quinone methides. This is confirmed in Figure 10b, where it can be observed that the samples containing Additive #5 have an overall lower intensity in the carbonyl region, which is where the contributions of oxidative products arising from the decomposition of hydroperoxides,[24] including esters, anhydrides, aliphatic and aromatic ketones, and carboxylic acids, are

located. In concordance, in the CH-stretching region, the intensity ratio of reference and degraded samples, as observed in the interval from 3100 to 2700 cm^{-1},[24,27] indicates a reduction of side chains degradation in the presence of Additive #5.

CONCLUSIONS

We report on the successful stabilization of organic solar cells using hindered phenols as stabilizing additives. Successful implementation of a stabilizing additive will depend on the polymer:fullerene system into which the additive is introduced, whereby the resulting ternary blend morphology and energy level alignment play the decisive role. Our work shows, on the example of stabilization of P3HT:PCBM system using a set of structurally varying hindered phenols, that it is possible to find such a compound which stabilizes the lifetime of the devices and at the same time does not disrupt its performance. Not all of the tested compounds were found suitable for use, due to the formation of trap states in the HOMO/LUMO gap of the photoactive layer. However, in the presence of octadecyl 3-(3,5-di-*tert*-butyl-4-hydroxyphenyl)propionate, also known under the product name Arenox A76, a drastic increase of the accumulated power generation (APG) of devices, by a factor of 3 compared to the reference without the stabilizing additive, was obtained. We suggest the hydrogen donation mechanism, in combination with the radical scavenging properties of the propionate type hindered phenols, to be responsible for the significant reduction of radicals within the photoactive layer, which can in turn stabilize the performance by decreasing the exciton recombination. However, as the possible morphological changes and trapping effects are strongly related to the specific polymer:fullerene system, one has to inspect the possible morphological and trapping issues for every such active layer system. The proof of the concept presented in this paper gives a general guideline on the important factors to be taken into consideration in choosing a fitting additive for any active layer system, which could prove to be of high importance for the commercialization of the organic solar cells, as it could enable the implementation of highly efficient materials regardless of their innate stability.

ASSOCIATED CONTENT

Supporting Information

Optical bandgaps of additives, optimization of additive concentration with regard to efficiency, solar cell parameters of the optimized cells, $I(V)$ curves for different concentrations of Additive #7, optical microscopy images of films with Additive #7 before and after degradation, FTIR analysis of the additive fraction in the films. This material is available free of charge via the Internet at http://pubs.acs.org.

AUTHOR INFORMATION

Corresponding Author

*E-mail: Vida.Turkovic@tu-ilmenau.de.

Present Address

Sebastian Engmann, National Institute of Standards and Technology, Gaithersburg, MD 20899, USA.

Author Contributions

The manuscript was written through contributions of all authors. All authors have given approval to the final version of the manuscript.

Notes

The authors declare no competing financial interest.

ACKNOWLEDGMENTS

The authors would like to thank Ms. Katrin Risch for recording the FTIR spectra and Ms. Doreen Schneider for additional CV-measurements. We thankfully acknowledge Dr. Solon Economopoulos for valuable discussion on cyclic voltammetry, and Mr. Ingo Werner from Reagens Deutschland GmbH for material samples. Financial support from the Federal State of Thuringia via the Landesgraduierten Stipendium, and Federal Ministry of Education and Research (BMBF) for funding of research projects EOS, PPP, and AIMS is gratefully acknowledged.

REFERENCES

(1) Green, M. A.; Emery, K.; Hishikawa, Y.; Warta, W.; Dunlop, E. D. Solar Cell Efficiency Tables (Version 40). *Prog. Photovoltaics* **2012**, *20*, 606−614.

(2) Nielsen, T. D.; Cruickshank, C.; Foged, S.; Thorsen, J.; Krebs, F. C. Business, Market and Intellectual Property Analysis of Polymer Solar Cells. *Sol. Energy Mater. Sol. Cells* **2010**, *94*, 1553−1571.

(3) Tanenbaum, D. M.; Hermenau, M.; Voroshazi, E.; Lloyd, M. T.; Galagan, Y.; Zimmermann, B.; Hosel, M.; Dam, H. F.; Jorgensen, M.; Gevorgyan, S. A.; Kudret, S.; Maes, W.; Lutsen, L.; Vanderzande, D.; Wuerfel, U.; Andriessen, R.; Roesch, R.; Hoppe, H.; Teran-Escobar, G.; Lira-Cantu, M.; Rivaton, A.; Uzunoglu, G. Y.; Germack, D.; Andreasen, B.; Madsen, M. V.; Norrman, K.; Krebs, F. C. The ISOS-3 Inter-Laboratory Collaboration Focused on the Stability of a Variety of Organic Photovoltaic Devices. *RSC Adv.* **2012**, *2*, 882−893.

(4) Jorgensen, M.; Norrman, K.; Krebs, F. C. Stability/Degradation of Polymer Solar Cells. *Sol. Energy Mater. Sol. Cells* **2008**, *92*, 686−714.

(5) Turkovic, V.; Engmann, S.; Egbe, D. A. M.; Himmerlich, M.; Krischok, S.; Gobsch, G.; Hoppe, H. Multiple Stress Degradation Analysis of the Active Layer in Organic Photovoltaics. *Sol. Energy Mater. Sol. Cells* **2014**, *120* (Part B), 654−668.

(6) Tanenbaum, D. M.; Dam, H. F.; Rosch, R.; Jorgensen, M.; Hoppe, H.; Krebs, F. C. Edge Sealing for Low Cost Stability Enhancement of Roll-to-Roll Processed Flexible Polymer Solar Cell Modules. *Sol. Energy Mater. Sol. Cells* **2012**, *97*, 157−163.

(7) Dennler, G.; Lungenschmied, C.; Neugebauer, H.; Sariciftci, N. S.; Latrèche, M.; Czeremuszkin, G.; Wertheimer, M. R. A New Encapsulation Solution for Flexible Organic Solar Cells. *Thin Solid Films* **2006**, *511−512*, 349−353.

(8) Jongwoon, P.; Hyogyun, H.; Youngmo, K.; Jongho, L.; Junghwan, P. In *2011 37th IEEE Photovoltaic Specialists Conference (PVSC 2011)*; IEEE: Seattle, WA, 2011; pp 001192−001194.

(9) Engmann, S.; Machalett, M.; Turkovic, V.; Rosch, R.; Radlein, E.; Gobsch, G.; Hoppe, H. Photon Recycling across a Ultraviolet-Blocking Layer by Luminescence in Polymer Solar Cells. *J. Appl. Phys.* **2012**, *112*, 034517−4.

(10) Alexander, M. D.; Specker, C. E.; Dudis, D. S. In *Reactive Intermediates in Organic and Biological Electrochemistry*; Peters, D. G., Schafer, H. J., Workentin, M. S., Yoshida, J., Eds.; The Electrochemical Society: Pennington, NJ, USA, 2001; pp 164−167.

(11) Mishra, S. P.; Palai, A. K.; Kumar, A.; Srivastava, R.; Kamalasanan, M. N.; Patri, M. Highly Air-Stable Thieno 3,2-B Thiophene-Thiophene-Thiazolo 5,4-D Thiazole-Based Polymers for Light-Emitting Diodes. *Macromol. Chem. Phys.* **2010**, *211*, 1890−1899.

(12) Manceau, M.; Bundgaard, E.; Carle, J. E.; Hagemann, O.; Helgesen, M.; Sondergaard, R.; Jorgensen, M.; Krebs, F. C. Photochemical Stability of Pi-Conjugated Polymers for Polymer Solar Cells: A Rule of Thumb. *J. Mater. Chem.* **2011**, *21*, 4132−4141.

(13) Kim, S. H.; Hwang, I.-W.; Jin, Y.; Song, S.; Moon, J.; Suh, H.; Lee, K. Long-Lived Bulk Heterojunction Solar Cells Fabricated with Photo-Oxidation Resistant Polymer. *Sol. Energy Mater. Sol. Cells* **2011**, *95*, 361−364.

(14) Grisorio, R.; Allegretta, G.; Mastrorilli, P.; Suranna, G. P. On the Degradation Process Involving Polyfluorenes and the Factors Governing Their Spectral Stability. *Macromolecules* **2011**, *44*, 7977−7986.
(15) Kim, H. J.; Park, J. H.; Lee, H. H.; Lee, D. R.; Kim, J.-J. The Effect of Al Electrodes on the Nanostructure of Poly(3-Hexylthiophene): Fullerene Solar Cell Blends During Thermal Annealing. *Org. Electron.* **2009**, *10*, 1505−1510.
(16) Rosch, R.; Tanenbaum, D. M.; Jorgensen, M.; Seeland, M.; Barenklau, M.; Hermenau, M.; Voroshazi, E.; Lloyd, M. T.; Galagan, Y.; Zimmermann, B.; Wurfel, U.; Hosel, M.; Dam, H. F.; Gevorgyan, S. A.; Kudret, S.; Maes, W.; Lutsen, L.; Vanderzande, D.; Andriessen, R.; Teran-Escobar, G.; Lira-Cantu, M.; Rivaton, A.; Uzunoglu, G. Y.; Germack, D.; Andreasen, B.; Madsen, M. V.; Norrman, K.; Hoppe, H.; Krebs, F. C. Investigation of the Degradation Mechanisms of a Variety of Organic Photovoltaic Devices by Combination of Imaging Techniques-the ISOS-3 Inter-Laboratory Collaboration. *Energy Environ. Sci.* **2012**, *5*, 6521−6540.
(17) Tsierkezos, N.; Ritter, U. Oxidation of Dopamine on Multi-Walled Carbon Nanotubes. *J. Solid State Electrochem.* **2012**, *16*, 2217−2226.
(18) Tsierkezos, N. G.; Ritter, U. Electrochemistry of Tris(2,2′-Bipyridine)Ruthenium(II) on Nitrogen-Doped Multi-Walled Carbon Nanotubes. *Chem. Sens.* **2013**, *3*, 8.
(19) Tsierkezos, N.; Ritter, U. Electrochemical Impedance Spectroscopy and Cyclic Voltammetry of Ferrocene in Acetonitrile/Acetone System. *J. Appl. Electrochem.* **2010**, *40*, 409−417.
(20) D'Andrade, B. W.; Datta, S.; Forrest, S. R.; Djurovich, P.; Polikarpov, E.; Thompson, M. E. Relationship between the Ionization and Oxidation Potentials of Molecular Organic Semiconductors. *Org. Electron.* **2005**, *6*, 11−20.
(21) Howell, J. O.; Goncalves, J. M.; Amatore, C.; Klasinc, L.; Wightman, R. M.; Kochi, J. K. Electron-Transfer from Aromatic-Hydrocarbons and Their Pi-Complexes with Metal - Comparison of the Standard Oxidation Potentials and Vertical Ionization-Potentials. *J. Am. Chem. Soc.* **1984**, *106*, 3968−3976.
(22) Reese, M. O.; Gevorgyan, S. A.; Jorgensen, M.; Bundgaard, E.; Kurtz, S. R.; Ginley, D. S.; Olson, D. C.; Lloyd, M. T.; Moryillo, P.; Katz, E. A.; Elschner, A.; Haillant, O.; Currier, T. R.; Shrotriya, V.; Hermenau, M.; Riede, M.; Kirov, K. R.; Trimmel, G.; Rath, T.; Inganas, O.; Zhang, F.; Andersson, M.; Tvingstedt, K.; Lira-Cantu, M.; Laird, D.; McGuiness, C.; Gowrisanker, S.; Pannone, M.; Xiao, M.; Hauch, J.; Steim, R.; DeLongchamp, D. M.; Roesch, R.; Hoppe, H.; Espinosa, N.; Urbina, A.; Yaman-Uzunoglu, G.; Bonekamp, J.-B.; van Breemen, A. J. J. M.; Girotto, C.; Voroshazi, E.; Krebs, F. C. Consensus Stability Testing Protocols for Organic Photovoltaic Materials and Devices. *Sol. Energy Mater. Sol. Cells* **2011**, *95*, 1253−1267.
(23) Zweifel, H. *Stabilization of Polymeric Materials*; Springer Verlag: Berlin, 1998.
(24) Manceau, M.; Rivaton, A.; Gardette, J.-L.; Guillerez, S.; Lemaitre, N. The Mechanism of Photo- and Thermooxidation of Poly(3-Hexylthiophene) (P3HT) Reconsidered. *Polym. Degrad. Stab.* **2009**, *94*, 898−907.
(25) Chambon, S.; Rivaton, A.; Gardette, J.-L.; Firon, M. Reactive Intermediates in the Initiation Step of the Photo-Oxidation of MDMO-PPV. *J. Polym. Sci., Part A: Polym. Chem.* **2009**, *47*, 6044−6052.
(26) Hintz, H.; Sessler, C.; Peisert, H.; Egelhaaf, H. J.; Chasse, T. Wavelength-Dependent Pathways of Poly-3-Hexylthiophene Photo-Oxidation. *Chem. Mater.* **2012**, *24*, 2739−2743.
(27) Abdou, M. S. A.; Holdcroft, S. Solid-State Photochemistry of Pi-Conjugated Poly(3-Alkylthiophenes). *Can. J. Chem.* **1995**, *73*, 1893−1901.
(28) Bolland, J. L.; Gee, G. Kinetic Studies in the Chemistry of Rubber and Related Materials. II. The Kinetics of Oxidation of Unconjugated Olefins. *Trans. Faraday Soc.* **1946**, *42*, 236−243.
(29) Pospíšil, J.; Nešpůrek, S. Chain-Breaking Stabilizers in Polymers: The Current Status. *Polym. Degrad. Stab.* **1995**, *49*, 99−110.
(30) Cooling, N. A.; Zhou, X. J.; Sales, T. A.; Sauer, S. E.; Lind, S. J.; Gordon, K. C.; Jones, T. W.; Burke, K. B.; Dastoor, P. C.; Belcher, W. J. A Study of the Factors Influencing the Performance of Ternary MEH-PPV:Porphyrin:PCBM Heterojunction Devices: Electronic Effects in Porphyrinoid Ternary Blend Bulk Heterojunction Photovoltaic Devices. *Sol. Energy Mater. Sol. Cells* **2012**, *98*, 308−316.
(31) Kuik, M.; Koster, L. J. A.; Wetzelaer, G. A. H.; Blom, P. W. M. Trap-Assisted Recombination in Disordered Organic Semiconductors. *Phys. Rev. Lett.* **2011**, *107*, 256805.
(32) Mutoro, E.; Luerßen, B.; Günther, S.; Janek, J. The Electrode Model System Pt(O2)|YSZ: Influence of Impurities and Electrode Morphology on Cyclic Voltammograms. *Solid State Ionics* **2009**, *180*, 1019−1033.
(33) Endres, F.; El Abedin, S. Z.; Borissenko, N. Probing Lithium and Alumina Impurities in Air- and Water Stable Ionic Liquids by Cyclic Voltammetry and in Situ Scanning Tunneling Microscopy. *Z. Phys. Chem.* **2006**, *220*, 1377−1394.
(34) Camaioni, N.; Tinti, F.; Franco, L.; Fabris, M.; Toffoletti, A.; Ruzzi, M.; Montanari, L.; Bonoldi, L.; Pellegrino, A.; Calabrese, A.; Po, R. Effect of Residual Catalyst on Solar Cells Made of a Fluorene-Thiophene-Benzothiadiazole Copolymer as Electron-Donor: A Combined Electrical and Photophysical Study. *Org. Electron.* **2012**, *13*, 550−559.
(35) Nikiforov, M. P.; Lai, B.; Chen, W.; Chen, S.; Schaller, R. D.; Strzalka, J.; Maser, J.; Darling, S. B. Detection and Role of Trace Impurities in High-Performance Organic Solar Cells. *Energy Environ. Sci.* **2013**, *6*, 1513−1520.
(36) Renaud, C.; Huang, C. H.; Lee, C. W.; Le Rendu, P.; Nguyen, T. P. Study of Trap States in Polyfluorene Based Devices by Using TSC Technique. *Thin Solid Films* **2008**, *516*, 7209−7213.
(37) Peet, J.; Kim, J. Y.; Coates, N. E.; Ma, W. L.; Moses, D.; Heeger, A. J.; Bazan, G. C. Efficiency Enhancement in Low-Bandgap Polymer Solar Cells by Processing with Alkane Dithiols. *Nat. Mater.* **2007**, *6*, 497−500.
(38) Qin, D. S.; Quan, W.; Liu, J. S.; Li, G. F.; Chen, L.; Zhang, J. D.; Yan, D. H. The Manageable Formation of the Gradient-Layered Polymer/Fullerene Blend Films Via the Addition of Bathocuproine and Their Applications in Organic Solar Cells. *Phys. Status Solidi A* **2012**, *209*, 1150−1156.
(39) Shin, M.; Kim, H.; Nam, S.; Park, J.; Kim, Y. Influence of Hole-Transporting Material Addition on the Performance of Polymer Solar Cells. *Energy Environ. Sci.* **2010**, *3*, 1538−1543.
(40) Schaffer, C. J.; Palumbiny, C. M.; Niedermeier, M. A.; Jendrzejewski, C.; Santoro, G.; Roth, S. V.; Müller-Buschbaum, P. A Direct Evidence of Morphological Degradation on a Nanometer Scale in Polymer Solar Cells. *Adv. Mater.* **2013**, *25*, 6760−6764.
(41) Collins, B. A.; Gann, E.; Guignard, L.; He, X.; McNeill, C. R.; Ade, H. Molecular Miscibility of Polymer-Fullerene Blends. *J. Phys. Chem. Lett.* **2010**, *1*, 3160−3166.
(42) Treat, N. D.; Brady, M. A.; Smith, G.; Toney, M. F.; Kramer, E. J.; Hawker, C. J.; Chabinyc, M. L. Interdiffusion of PCBM and P3HT Reveals Miscibility in a Photovoltaically Active Blend. *Adv. Energy Mater.* **2011**, *1*, 82−89.
(43) Müller, C.; Ferenczi, T. A. M.; Campoy-Quiles, M.; Frost, J. M.; Bradley, D. D. C.; Smith, P.; Stingelin-Stutzmann, N.; Nelson, J. Binary Organic Photovoltaic Blends: A Simple Rationale for Optimum Compositions. *Adv. Mater.* **2008**, *20*, 3510−3515.
(44) van Bavel, S. S.; Sourty, E.; de With, G.; Loos, J. Three-Dimensional Nanoscale Organization of Bulk Heterojunction Polymer Solar Cells. *Nano Lett.* **2009**, *9*, 507−513.
(45) Ray, B.; Alam, M. A. Random vs Regularized OPV: Limits of Performance Gain of Organic Bulk Heterojunction Solar Cells by Morphology Engineering. *Sol. Energy Mater. Sol. Cells* **2012**, *99*, 204−212.
(46) Dibb, G. F. A.; Jamieson, F. C.; Maurano, A.; Nelson, J.; Durrant, J. R. Limits on the Fill Factor in Organic Photovoltaics: Distinguishing Nongeminate and Geminate Recombination Mechanisms. *J. Phys. Chem. Lett.* **2013**, *4*, 803−808.

(47) Aguirre, A.; Meskers, S. C. J.; Janssen, R. A. J.; Egelhaaf, H. J. Formation of Metastable Charges as a First Step in Photoinduced Degradation in Pi-Conjugated Polymer: Fullerene Blends for Photovoltaic Applications. *Org. Electron.* **2011**, *12*, 1657−1662.
(48) Turkovic, V.; Engmann, S.; Gobsch, G.; Hoppe, H. Methods in Determination of Morphological Degradation of Polymer:Fullerene Solar Cells. *Synth. Met.* **2012**, *161*, 2534−2539.
(49) Bertho, S.; Janssen, G.; Cleij, T. J.; Conings, B.; Moons, W.; Gadisa, A.; D'Haen, J.; Goovaerts, E.; Lutsen, L.; Manca, J.; Vanderzande, D. Effect of Temperature on the Morphological and Photovoltaic Stability of Bulk Heterojunction Polymer:Fullerene Solar Cells. *Sol. Energy Mater. Sol. Cells* **2008**, *92*, 753−760.
(50) Conings, B.; Bertho, S.; Vandewal, K.; Senes, A.; D'Haen, J.; Manca, J.; Janssen, R. A. J. Modeling the Temperature Induced Degradation Kinetics of the Short Circuit Current in Organic Bulk Heterojunction Solar Cells. *Appl. Phys. Lett.* **2010**, *96*, 163301.
(51) Reese, M. O.; Nardes, A. M.; Rupert, B. L.; Larsen, R. E.; Olson, D. C.; Lloyd, M. T.; Shaheen, S. E.; Ginley, D. S.; Rumbles, G.; Kopidakis, N. Photoinduced Degradation of Polymer and Polymer-Fullerene Active Layers: Experiment and Theory. *Adv. Funct. Mater.* **2010**, *20*, 3476−3483.
(52) Distler, A.; Sauermann, T.; Egelhaaf, H.-J.; Rodman, S.; Waller, D.; Cheon, K.-S.; Lee, M.; Guldi, D. M. The Effect of PCBM Dimerization on the Performance of Bulk Heterojunction Solar Cells. *Adv. Energy Mater.* **2014**, *4*, 1−6.
(53) Abdou, M. S. A.; Orfino, F. P.; Son, Y.; Holdcroft, S. Interaction of Oxygen with Conjugated Polymers: Charge Transfer Complex Formation with Poly(3-Alkylthiophenes). *J. Am. Chem. Soc.* **1997**, *119*, 4518−4524.
(54) Drori, T.; Holt, J.; Vardeny, Z. V. Optical Studies of the Charge Transfer Complex in Polythiophene/Fullerene Blends for Organic Photovoltaic Applications. *Phys. Rev. B* **2010**, *82*, 075207.
(55) Cook, S.; Furube, A.; Katoh, R. Matter of Minutes Degradation of Poly(3-Hexylthiophene) under Illumination in Air. *J. Mater. Chem.* **2012**, *22*, 4282−4289.
(56) Hintz, H.; Egelhaaf, H. J.; Luer, L.; Hauch, J.; Peisert, H.; Chasse, T. Photodegradation of P3HT-a Systematic Study of Environmental Factors. *Chem. Mater.* **2011**, *23*, 145−154.
(57) Pospíšil, J.; Nešpůrek, S.; Zweifel, H.; Kuthan, J. Photo-Bleaching of Polymer Discoloration Caused by Quinone Methides. *Polym. Degrad. Stab.* **2002**, *78*, 251−255.
(58) Klemchuk, P. P.; Horng, P.-L. Transformation Products of Hindered Phenolic Antioxidants and Colour Development in Polyolefins. *Polym. Degrad. Stab.* **1991**, *34*, 333−346.
(59) Pacios, R.; Chatten, A. J.; Kawano, K.; Durrant, J. R.; Bradley, D. D. C.; Nelson, J. Effects of Photo-Oxidation on the Performance of Poly 2-Methoxy-5-(3 ′,7 ′-Dimethyloctyloxy)-1,4-Phenylene Vinylene: 6,6 -Phenyl C-61-Butyric Acid Methyl Ester Solar Cells. *Adv. Funct. Mater.* **2006**, *16*, 2117−2126.
(60) Bauld, R.; Fleury, L. M.; Van Walsh, M.; Fanchini, G. Correlation between Density of Paramagnetic Centers and Photovoltaic Degradation in Polythiophene-Fullerene Bulk Heterojunction Solar Cells. *Appl. Phys. Lett.* **2012**, *101*, 103306−4.
(61) Krebs, F. C.; Carlé, J. E.; Cruys-Bagger, N.; Andersen, M.; Lilliedal, M. R.; Hammond, M. A.; Hvidt, S. Lifetimes of Organic Photovoltaics: Photochemistry, Atmosphere Effects and Barrier Layers in ITO-MEHPPV:PCBM-Aluminium Devices. *Sol. Energy Mater. Sol. Cells* **2005**, *86*, 499−516.
(62) Peters, C. H.; Sachs-Quintana, I. T.; Kastrop, J. P.; Beaupré, S.; Leclerc, M.; McGehee, M. D. High Efficiency Polymer Solar Cells with Long Operating Lifetimes. *Adv. Energy Mater.* **2011**, *1*, 491−494.
(63) Pospisil, J.; Nespurek, S.; Zweifel, H. In *Chemistry and Technology of Polymer Additives*; Al-Malaika, S., Golovoy, A., Wilkie, C. A., Eds.; Blackwell Science Ltd.: Oxford, UK, 1999; Chapter 3, pp 36−61.
(64) Pospisil, J. In *Oxidation Inhibition in Organic Materials*; Pospisil, J., Klemchuk, P., Eds.; CRC Press: Boca Raton, USA, 1990; Chapter 1.
(65) Billingham, N. C.; Calvert, P. D.; Manke, A. S. Solubility of Phenolic Antioxidants in Polyolefins. *J. Appl. Polym. Sci.* **1981**, *26*, 3543−3555.
(66) Gugumus, F. In *Plastics Additives Handbook*; Gachter, R., Muller, H., Klemchuk, P. P., Eds.; Hanser/Gardner Publications, Inc.: Cincinnati, OH, 1993; Chapter 1, pp 1−104.
(67) Zweifel, H. In *Polymer Durability - Degradation, Stabilization, and Lifetime Prediction*; Clough, R. L., Billingham, N. C., Gillen, K. T., Eds.; American Chemical Society: Washington, DC, 1996; Chapter 25, pp 375−397.
(68) Manceau, M.; Gaume, J.; Rivaton, A.; Gardette, J.-L.; Monier, G.; Bideux, L. Further Insights into the Photodegradation of Poly(3-Hexylthiophene) by Means of X-Ray Photoelectron Spectroscopy. *Thin Solid Films* **2010**, *518*, 7113−7118.
(69) Norrman, K.; Larsen, N. B.; Krebs, F. C. Lifetimes of Organic Photovoltaics: Combining Chemical and Physical Characterisation Techniques to Study Degradation Mechanisms. *Sol. Energy Mater. Sol. Cells* **2006**, *90*, 2793−2814.